BeFo

STIFTELSEN BERGTEKNISK FORSKNING
ROCK ENGINEERING RESEARCH FOUNDATION

OPTIMIZATION OF TIME DOMAIN INDUCED POLARIZATION DATA ACQUISITION AND SPECTRAL INFORMATION CONTENT

Per-Ivar Olsson

BeFo Report 162

STIFTELSEN BERGTEKNISK FORSKNING
ROCK ENGINEERING RESEARCH FOUNDATION

OPTIMIZATION OF TIME DOMAIN INDUCED POLARIZATION DATA ACQUISITION AND SPECTRAL INFORMATION CONTENT

Optimering av mätförfarande och frekvensberoende informationsinnehåll för undersökningar av geoelektrisk uppladdningsförmåga

Per-Ivar Olsson, Lund University

BeFo Report 162
Stockholm 2024
ISSN 1104 – 1773
ISRN BEFO-R—162—SE

This report is a representation of the Licentiate Thesis “Optimization of time domain induced polarization data acquisition and spectral information content”.
Division of Engineering Geology, Lund University, 2016.
ISBN (Print) 978-91-7623-671-0
ISBN (Pdf) 978-91-7623-672-7
ISRN LUTVDG/(TVTG-1035)/1-94/(2016)
This BeFo report is published with the permission of the author.

Preface

Unforeseen ground conditions are a risk factor often leading to delays and significant additional costs in connection with urban underground infrastructure construction work. The main geological hazards for these construction works are unstable rock, large inflow of groundwater and waste deposits The purpose of this research project is to adapt and optimize geophysical methods for reducing the uncertainty related to these hazards and to some extent identify and delineate them. Specifically, this project has developed and adapted the resistivity-induced polarization (DCIP) imaging method for use in infrastructural developments in urban environments.

This report is in parts based on a licentiate thesis; the work was supported by a reference group consisted of Lee Slater, Andy Binley, William Powrie, Robert Sturk, Thomas Günther, Roger Wisén, Andreas Pfaffhuber, Ulf Håkansson, Malin Ohlin, Staffan Hintze, Christel Karlsson, Thomas Sträng, Nils Otters and Per Tengborg.

The work was co-funded by Formas - The Swedish Research Council for Environment, Agricultural Sciences and Spatial Planning, SBUF - The Development Fund of the Swedish Construction Industry, Hakon Hansson foundation, Ernhold Lundström foundation and BeFo - Swedish Rock Engineering Research Foundation.

Stockholm

Patrik Vidstrand

Förord

Oförutsedda markförhållanden är en riskfaktor som ofta leder till förseningar och betydande merkostnader i samband med infrastrukturprojekt under mark. De viktigaste geologiska riskerna för dessa byggprojekt är instabilt berg, stort inflöde av grundvatten och avfallsdeponier. Syftet med detta forskningsprojekt är att anpassa och optimera geofysiska metoder för att minska osäkerheten kopplad till dessa risker och i viss mån kunna identifiera och avgränsa dem. Närmare bestämt har detta projekt utvecklat och anpassat resistivitet-inducerad polarisationsmetoden (DCIP) för användning som förundersökningsmetod för infrastrukturutveckling under mark i urbana miljöer.

Rapporten är till delar baserad på en licentiatuppsats; referensgruppen för projektet bestod av Lee Slater, Andy Binley, William Powrie, Robert Sturk, Thomas Günther, Roger Wisén, Andreas Pfaffhuber, Ulf Håkansson, Malin Ohlin, Staffan Hintze, Christel Karlsson, Thomas Sträng, Nils Otters och Per Tengborg.

Projektet är samfinansierat av Formas - Forskningsrådet för miljö, areella näringar och samhällsbyggande, SBUF - Svenska Byggbranschens Utvecklingsfond, Hakon Hansson stiftelse och Ernhold Lundström stiftelse och BeFo.

Stockholm

Patrik Vidstrand

Summary

The need for detailed subsurface information is increasing due to city expansion and infill projects as well as subsurface construction projects. One common method for acquiring this geo-information is the direct current resistivity and time domain induced polarization method (DCIP) that measures the electrical resistivity and chargeability of the subsurface. The work presented in this report demonstrates that the usefulness of the DCIP method can be improved. Field time and cost efficiency is increased by means of waveform optimization and investigations of the effect of different current pulse on-time duration. Furthermore, post processing efficiency is increased as a result of improved data quality and reliability. Additionally, the available spectral information from DCIP surveys is substantially increased by enabling extraction of the IP response closer to the pulse than was previously possible. In combination with more accurate removal of background drift potential, which improves data quality at late times, the spectral information is further increased. In total, these optimizations increase the usefulness of the resistivity and (spectral) time domain induced polarization method and can hopefully contribute to spreading and intensifying its use for acquiring qualified subsurface information.

Keywords: induced polarization, resistivity, signal processing, geophysics

Sammanfattning

Behovet av detaljerad undermarksinformation ökar ständigt på grund av stadsexpansions-, förtätnings-, och infrastrukturprojekt under mark. En vanlig metod för att erhålla sådan geo(fysisk)-information är resistivitet och inducerad polarisation metoden (DCIP) vilken mäter markens elektriska motstånd och uppladdningsförmåga. Arbetet som presenteras i denna rapport visar att användbarheten av DCIP metoden kan förbättras. Fälttids- och kostnadseffektivitet ökas med hjälp av optimering av utsänd strömvågform samt undersökningar av effekten av olika strömpulstider. Utöver detta ökas effektiviteten för efterbearbetning av data till följd av en förbättrad datakvalitet och tillförlitlighet. Dessutom ökas den tillgängliga spektrala information från DCIP undersökningar avsevärt genom att möjliggöra extraktion av IP-information närmare strömpulsstegen än vad som tidigare varit möjligt. I kombination med en mer avancerad borttagning av bakgrundsvariationer i uppmätt potential, vilket förbättrar datakvaliteten vid sena IP-tider, utökas den spektrala IP informationen avsevärt. Sammantaget ökar dessa framsteg användbarheten av resistivitet och (spektral) inducerad polarisation metoden och kan förhoppningsvis bidra till att sprida och intensifiera dess användning för att förvärva kvalificerad undermarksinformation.

Nyckelord: inducerad polarisation, resistivitet, signalbehandling, geofysik

Contents

1 Introduction

The need for detailed information of the subsurface is increasing due to city expansion and infill projects as well as subsurface construction projects (e.g. tunnelling). One common method for acquiring this geo-information is the direct current resistivity and time domain induced polarization method (DCIP) which measures the electrical resistivity and chargeability of the subsurface (Dahlin, 2001; Loke et al., 2013). This report summarizes selected work on developing and increasing the usefulness of the DCIP method with focus on the induced polarization.

Electrical resistivity tomography (ERT) has been successfully used in a wide range of subsurface applications (Loke et al., 2013) such as environmental and engineering (Auken et al., 2014; Dahlin et al., 1999), hydrogeological (Auken et al., 2006; Fetter, 2001; Leroux and Dahlin, 2005) and archaeological (Argote-Espino et al., 2013; Florsch et al., 2011). However, different subsurface materials can have the same resistivity (Glover, 2015) and thus is it not possible to differentiate them when only using the resistivity information. This makes the chargeability information especially valuable since it can be measured simultaneously with the resistivity with little or no extra effort and the materials can have the same value for resistivity but different values for the chargeability. Hence, having two parameters reduces the ambiguity when relating the DCIP measurements to processes and geology. This reduction in ambiguity has been demonstrated for several applications, such as landfill mapping (Dahlin et al., 2010; Leroux et al., 2007) and lithology mapping (Kemna et al., 2004; Slater and Lesmes, 2002) and microbial activities (Slater et al., 2008),

The induced polarization phenomenon can be further evaluated by considering its frequency dependency, the spectral information. The frequency dependency is described with different models and, depending on the choice of model, additional parameters can be retrieved from the chargeability measurements so that the possible ambiguity can be reduced even more. The use of spectral IP information in engineering applications is still limited but there are several examples of research where the spectral information has proven useful. For example for aquifer characterization (Revil et al., 2015; Slater and Glaser, 2003), mapping geochemical changes (Doetsch et al., 2015a), permafrost monitoring (Doetsch et al., 2015b) and landfill mapping (Gazoty et al., 2013, 2012a, 2012b).

Even if different levels of chargeability information generally can be retrieved from DCIP surveys, often only the resistivity parameters are evaluated in applied engineering investigations. This has several explanations, for example: older instruments with limited capability of successfully measuring the chargeability are still in use and knowledge of how the chargeability information should be interpreted could be missing. Another important factor is related to data quality, since the induced polarization measurement have much lower signal-to-noise ratio compared to the resistivity measurements, the data quality can be poor. Using the data would require more time for manual filtering of the data, and thus more money than can be allocated to make use of the chargeability data. This calls for an assessment on how to generally improve the quality of the acquired induced polarization data, and automated ways of data quality assessment and data filtering.

This spectral evaluation in turn demands a wide time-range of chargeability information (e.g. from one millisecond to several seconds) and even higher data quality than the regular “one parameter evaluation”. Hence smart processing of the DCIP data is needed in order to allow a more widespread use of the method. Time and cost efficiency of spectral DCIP measurements is also limiting the usefulness of the method. The field measurements can require thousands of readings, where more data stacking and longer current transmission pulses may be required compared to what would be used in a regular DCIP survey. Thus there is a need for optimizing the measurement procedure to reduce the time and costs related to the field surveys.

1.1 Aim, objective and limitations

The aim of this study is to increase the usefulness of the DCIP method by developing the data acquisition and processing methodology. Therefore, the objectives of this study are to reduce acquisition time and costs, to increase data (spectral) information content, reliability and quality and to reduce the time and cost for data processing.

This work has not considered any other field surveying or geophysical method than the direct current resistivity and time domain induced polarization method. Additionally, the handling of electromagnetic coupling has not been considered as a part of this work except for applying an improved field procedure (Dahlin and Leroux, 2012). Furthermore, the work has focused on developing the time domain measurement technique rather than the frequency domain counterpart. Due to this is only a very brief overview given regarding the frequency domain measurements.

2 The DCIP method

DCIP measurements are carried out by injecting current into the subsurface between two electrodes while measuring the potential between one or several other pairs of electrodes (Figure 1) (Fink, 1990; Sumner, 2012; Zonge et al., 2005). The aim of the measurements is to get information of the electrical resistivity and chargeability of the subsurface. Information from different sub volumes of the subsurface is retrieved by repeating the measurements with different electrode combinations. With electrode combinations arranged along a line, one- or two-dimensional, depending on what combinations are used, information of the subsurface below the line can be retrieved. If the combinations instead cover an area it is possible to recover a three-dimensional information volume (Loke and Barker, 1996).

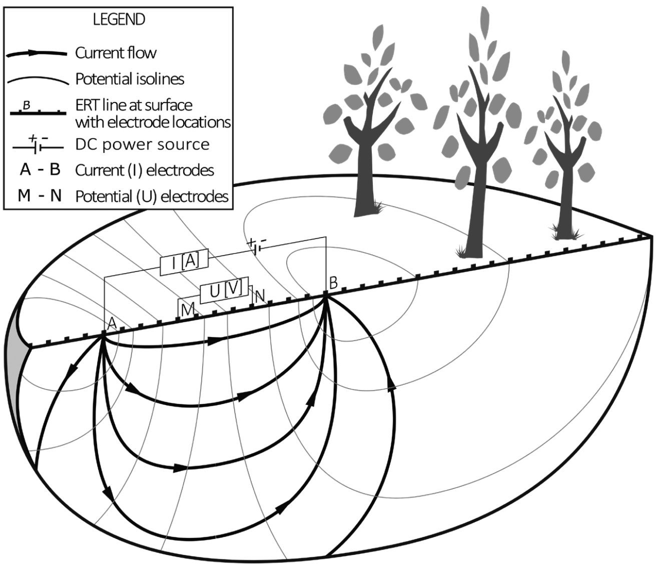

Figure 1. Schematic overview of 2D DCIP measurement principle on a homogenous subsurface. Original image provided by Nijland et al. (2010).

2.1 Resistivity

The resistivity (ρ, unit Ωm) is a material property that quantifies to what extent the material is opposing the flow of electrical current.

From the measurements of the current (I) and potential (V_{DC}, Figure 2) is it possible to calculate the resistance (R) of the subsurface through Ohm's law:

$$R = \frac{V_{DC}}{I}$$

By also taking into account the geometry of the electrode placements (geometric factor, K) one may retrieve the apparent resistivity (ρ_a), which only corresponds to the true resistivity of the subsurface if it is homogenous and isotropic.

$$\rho_a = K\frac{V_{DC}}{I}$$

where

$$K = 2\pi(r_{AM}^{-1} - r_{BM}^{-1} - r_{AN}^{-1} + r_{BN}^{-1})^{-1}$$

and r denotes the different distances between current (A and B) and potential (M and N) electrodes. If the subsurface has a heterogeneous distribution of resistivities is it necessary to conduct a more advanced interpretation of the measurements to retrieve the resistivity of the subsurface, see 2.5 Inversion.

2.2 Chargeability

The chargeability (m_0, unit mV/V) is a material property that quantifies the capacity of the material to store energy.

The chargeability is defined as the ratio between the measured voltage following a sudden change in current ($V_{IP,0}$, Figure 2), normalized with the measured potential before the current change (V_{DC}) (Seigel, 1959):

$m_0 = \frac{V_{IP,0}}{V_{DC}}$.

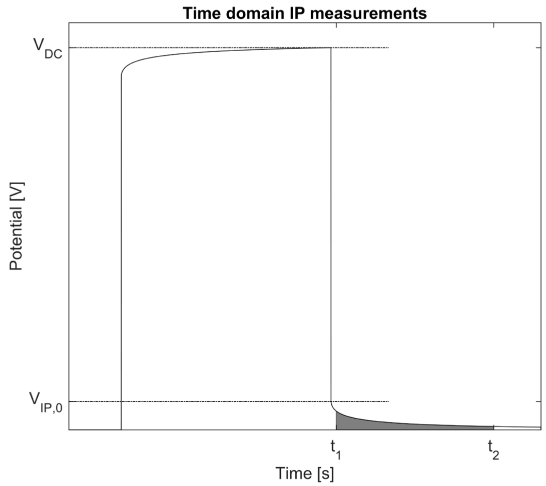

Figure 2. Theoretical full waveform potential for DCIP measurements with indication of parameters important for the data evaluation.

The chargeability is in time-domain determined by considering the transient potential response of the subsurface following a change in the injected current (Figure 2). It can be evaluated in several ways: for chargeability only (definition), for the mean chargeability within a given time interval (integral chargeability, m_{int}):

$$m_{int} = \frac{1}{V_{DC}\Delta t}\int_{t_1}^{t_2} V(t)dt$$

or for normalized integral chargeability (normalized with resistivity, see Slater and Lesmes (2002)) corresponding to surface polarization (Binley, 2015). Furthermore, the frequency characteristics of the potential response can be considered (spectral chargeability) by using different models for describing the shape (Figure 3) of the IP response (Johnson, 1984; Tombs, 1981), for example the Cole-Cole model in time-domain is described by (Florsch et al., 2011; Pelton et al., 1978; Revil et al., 2015):

$$V_{IP}(t) = m_0 \sum_{j=0}^{\infty} (-1)^j \left(\frac{t}{\tau}\right)^{jc} \Gamma(1+jc)^{-1}$$

for relaxation time (τ), frequency exponent (c) and Euler's Gamma function (Γ):

$\Gamma(x) = \int_0^\infty y^{x-1} e^{-u}\, dy$.

Analogous to resistivity and apparent resistivity it is not possible to directly retrieve the chargeability of the subsurface from the DCIP measurements unless it is homogenous in terms of chargeability, thus normally inversion is needed.

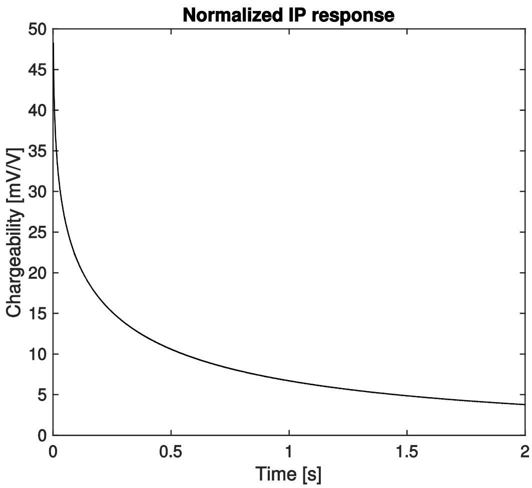

Figure 3. A normalized IP response generated from the modelled measurement seen in Figure 4.

2.3 Measurement waveforms

The current waveform injected into the ground differs depending on whether the measurements are conducted in time or frequency domain. Time domain measurements consider changes with time, while frequency domain measurements consider at what frequencies the changes take place. The two methods are theoretically equivalent but differ in terms of measurement technique and actual capability to resolve the spectral IP parameters (Binley, 2015).

2.3.1 Time domain

Time domain measurements typically inject a 50% duty cycle square current waveform with constant current (Figure 4). The polarity of the current is reversed every pulse in order to remove background potentials superimposed on the signal measured between the receiver electrodes, caused by electrode polarization effects (Binley, 2015). Thus, at least two pulses with opposite sign are injected. This pulse train can be repeated (stacked) to retrieve multiple readings of the potential response and reduce the influence of noise (see 3 Measurement challenges).

The potential readings (V_{DC}, Figure 2) for calculating resistivity are taken as an average potential at the end of each current injection so that the potential has had time to stabilize and that prominent IP responses likely have worn off. For IP the potential readings are taken during the current off-time and the potential is normally averaged within predefined windows, starting at a fixed delay time after the current pulses. The time windows have increasing lengths and are normally chosen as multiples of the time period of the household power grid frequency (i.e. 50 Hz and 20 milliseconds in Sweden) to average out harmonic noise. The integral chargeability is determined as a weighted sum of the IP windows while for spectral IP all windows and timing information is required for the inversion.

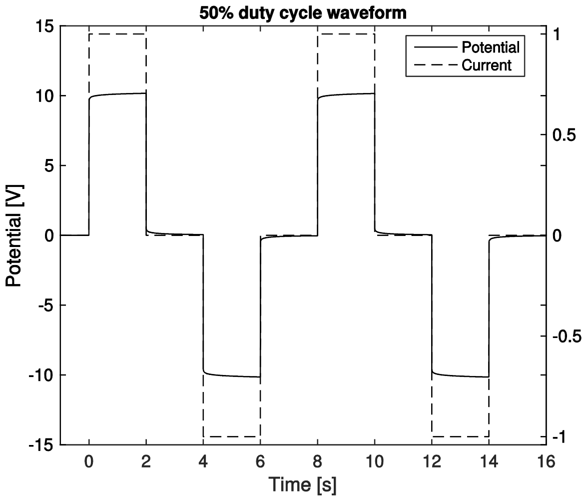

Figure 4. Injected current and modelled measured potential for the 50% duty-cycle waveform used for time domain DCIP measurements. Two stacks is achieved with 4 pulses and a current on-time of 2s. The corresponding stacked, averaged and normalized IP response can be seen in Figure 3.

2.3.2 Frequency domain

In frequency domain, current with a sine waveform of different frequencies is transmitted while the resistivity and IP information is retrieved as the amplitude and phase shift of the measured potential respectively (Binley, 2015; Florsch et al., 2011). By having a narrow passband filter corresponding to the frequency of the current transmitted it is possible to filter out background drift (~DC), harmonic noise (by avoiding transmitting at harmonic noise frequencies or its harmonics) and in part also the spikes.

2.4 Time or frequency domain?

Many technical measurement issues related to different noise sources (see 3 Measurement challenges) can be avoided if the measurements are carried out in frequency domain instead of in time domain. Furthermore, it should be noted that extracting spectral IP parameters (e.g. Cole-Cole) from time-domain measurements theoretically assumes that all polarization processes have been saturated and that early decay times (<400 milliseconds) might be affected by non-desirable processes such as Maxwell-Wagner polarization and electromagnetic coupling (Revil et al., 2015). However, the frequency domain measurements are highly time consuming compared to the time domain counterpart and consequently rarely used in commercial engineering and environmental applications but mainly used for research purposes. Since this work is aiming at techniques that can be expected to be adapted for routine practical applications it focuses on developing time domain measurements and on pushing the limit of the available spectral IP information from direct current resistivity and time domain induced polarization measurements.

2.5 Inversion

Inversion is an iterative process that aims to find a parameter model that gives synthetic measurements (forward response) that are similar to the real measurements. During the process the measured data are compared with the forward response for a known distribution of parameters (e.g. resistivity and chargeability) and the parameter values are changed until the responses are similar to the real measurements (Binley, 2015; Günther et al., 2006; Loke and Barker, 1996; Rücker et al., 2006).

Depending on the type of inversion, different numbers of parameters are used for describing the model space. For example, with the spectral chargeability Cole-Cole model four parameters are used: resistivity, chargeability, relaxation time and frequency exponent, where the latter three describes the shape of the IP response (Fiandaca et al., 2013, 2012; Hönig and Tezkan, 2007).

The time domain spectral chargeability inversion software described by Fiandaca et al. (2012 and 2013) models the waveform of current and potential, computes the forward response in frequency domain and transforms the response into time domain for comparing the measured data with the modelled response.

3 Measurement challenges

In field DCIP measurements the measured potentials are a mix of different sources (Figure 5), including the desired ground response of the current injection:

$$u_{measured} = u_{response} + u_{drift} + u_{harmonic\ noise} + u_{spikes} + u_{other}$$

To get an accurate determination of the potential response ($u_{response}$) it is essential to determine and compensate for as many of these sources as possible.

Figure 5. Different kinds of known sources that affect the measured potential and their typical signal characteristics: electrical fence - spikes (top left), power grid – harmonic noise (top right), tram running on DC – background drift (bottom left), DCIP instrument – square pulse train (bottom right).

3.1 Background drift

Background drift in DCIP data can have multiple origins, for example natural potential difference in the subsurface, natural electrode polarization (can be reduced using so called non-polarizable electrodes) and current induced electrode polarization (if using same electrodes for injecting current and measuring potentials). The drift is seen as a slow changing potential variation in the full waveform potential recording (Figure 6). If not corrected for, the drift can corrupt both resistivity and chargeability data but it is especially the tail of the IP response that is sensitive, due to its low signal-to-noise ratio, and thus mainly the spectral IP is affected. The correction for the drift is commonly done with a linear approximation (Dahlin et al., 2002; Peter-Borie et al., 2011).

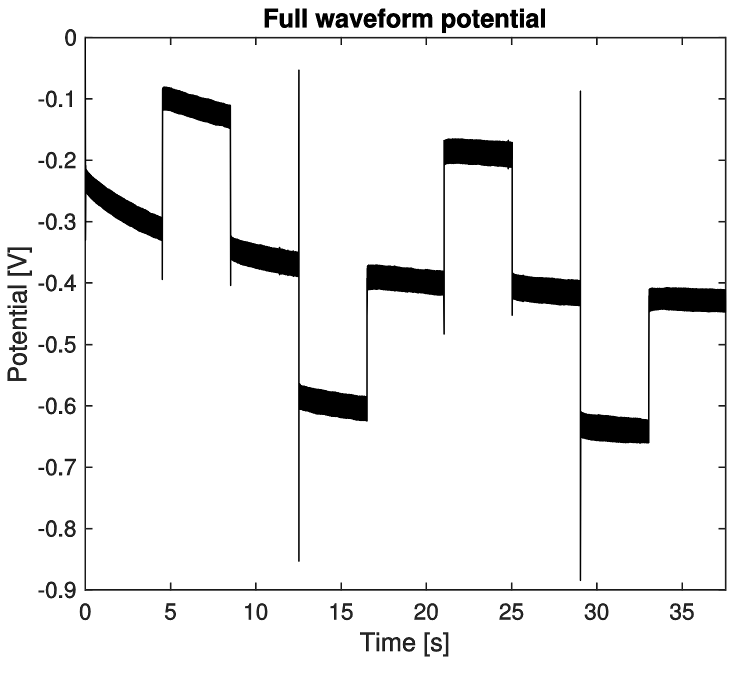

Figure 6. Example of full waveform potential recording that exhibits a clear background drift.

3.2 Spikes

Spikes (Figure 7) originating from anthropogenic sources, such as electrical fences for livestock management, can be registered by DCIP measurements. These spikes can cause problems when extracting DC (resistivity) and especially, due to its low signal-to-noise ratio, IP information from measured field data.

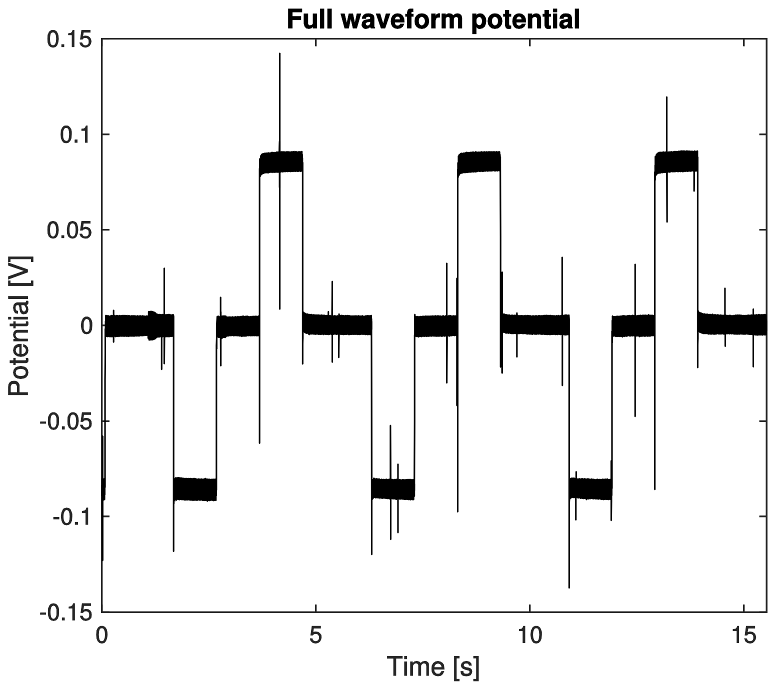

Figure 7. Example of full waveform potential recording with multiple spikes present.

3.3 Harmonic noise

Harmonic noise originates from the power supply sources oscillating at a base frequency (e.g. 50 Hz or 60 Hz) and harmonics of this base frequency (Figure 8 and Figure 9). In DCIP processing today, this is handled by averaging and gating over a full period of the known base frequency (e.g. 1/50 s or 1/60 s) for suppressing household power supply frequencies at 50 Hz and its harmonics. However, the need for long gates causes a loss of early IP response information close to current pulse change and thus makes it more difficult to resolve spectral parameters. This is especially severe when conducting field measurements close to electric railways in some countries (e.g. Austria, Germany, Norway, Sweden, Switzerland and USA) where the frequency of the power supply for the trains are even lower (16 2/3 Hz or 25 Hz).

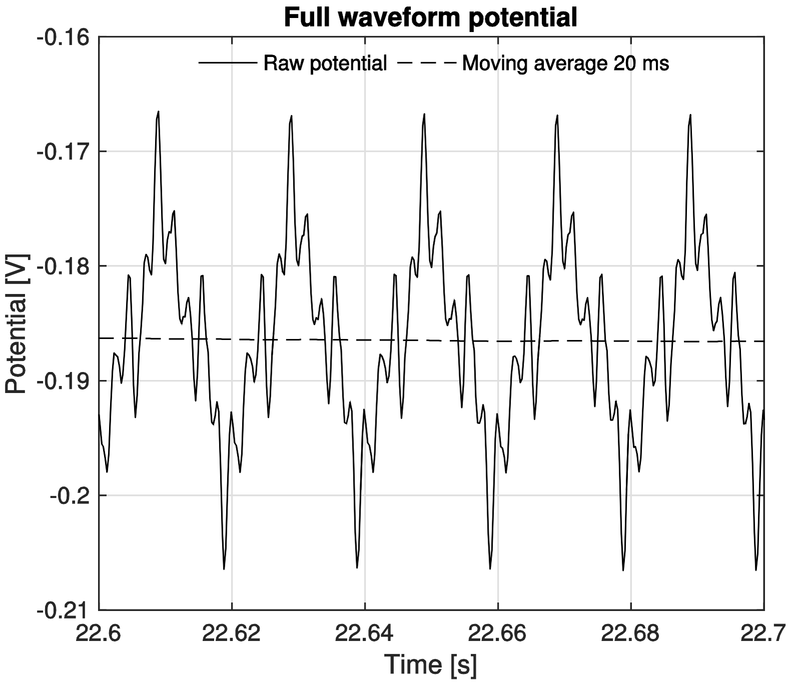

Figure 8. A magnification of the full waveform potential recording in Figure 6 and a moving average (20 millisecond window) version of the same signal. With the magnification the harmonic oscillations are clearly visible. The main oscillation has a time period of around 20 milliseconds.

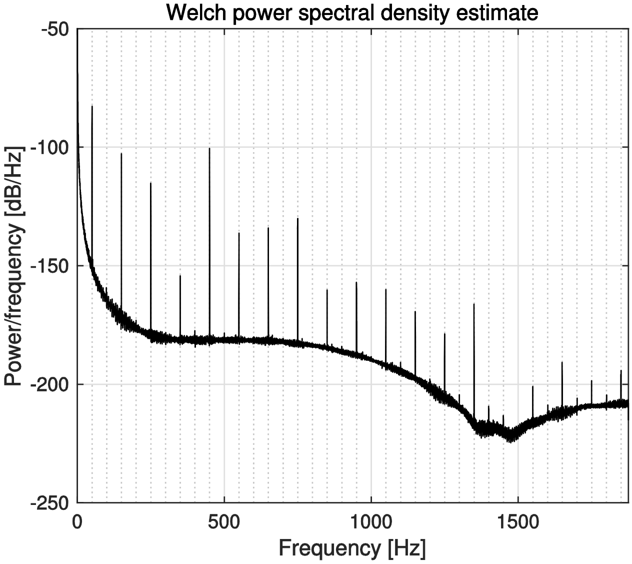

Figure 9. Welch power spectral density estimate for the time domain raw potential signal shown in Figure 6. The periodic reoccurring energy peaks suggest that harmonic noise from the power grid is present in the signal.

3.4 Electromagnetic coupling

Field surveys conducted with multicore cables where the potential and current wires are bulked in the same cable, as shown in Figure 1, generally suffer from different forms of electromagnetic (EM) coupling (Dahlin and Leroux, 2012). Handling of EM coupling is not a focus of this work, hence only a very brief overview is given here, but it should be noted that the coupling generally increases for longer arrays, lower resistivities and higher frequencies (Butler, 2005).

3.4.1 Capacitive coupling

Capacitive coupling can be defined as current leaks from high-potential surfaces or conductors to low-potential surfaces or conductors (Dahlin and Leroux, 2012). With a single multicore cable three main capacitive couplings can occur (Dahlin and Leroux, 2012; Radic, 2004): coupling between current and potential wire, coupling between the different current wires and coupling between current wire and the subsurface.

The main coupling effect is the one occurring between current and potential wires (Radic, 2004). One method to reduce this coupling is to increase the distance between the current and potential wires by using two multicore cables (Figure 10), one for current transmission and the other for potential measurements (Dahlin and Leroux, 2012).

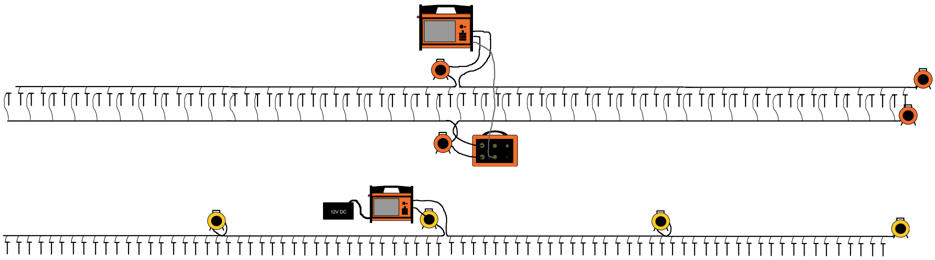

Figure 10. Example of measurement setup with two multicore cables (top). One cable and every second electrode is used for current injections while the remaining cable and electrodes are used for measuring potentials. By increasing the distance between current and potential wire the capacitive coupling between the two is reduced. Example of the traditional setup is provided for comparison (bottom). Image adapted from original by Torleif Dahlin.

3.4.2 Inductive coupling

Inductive coupling operates through magnetic fields and thus differs in origin from the capacitive coupling. It is possible to compensate for this coupling by means of modeling and also include it in the inversion (Ingeman-Nielsen and Baumgartner, 2006) but since focus of this work has been elsewhere this has not been considered in this work.

4 Main results

4.1 100% duty cycle current waveform

These results concern current waveform optimization to reduce acquisition time and increase signal-to-noise ratio.

Combined resistivity and time-domain direct current induced polarization (DCIP) measurements are traditionally carried out with a 50% duty cycle current waveform, taking the resistivity measurements during the on-time and the IP measurements during the off-time. One drawback with this method is that only half of the acquisition time is available for resistivity and IP measurements, respectively. In this paper, this limitation is solved by using a current injection with 100% duty cycle (Figure 11) and also taking the IP measurements in the on-time. With numerical modeling of current waveforms with 50% and 100% duty cycles the paper shows that the waveforms have comparable sensitivity for the spectral Cole–Cole parameters and that signal level is increased up to a factor of two if the 100% duty cycle waveform is used. The inversion of field data acquired with both waveforms (Figure 12) confirms the modeling results and shows that it is possible to retrieve similar inversion models with either of the waveforms when inverting for the spectral Cole–Cole parameters with the waveform of the injected current included in the forward computations.

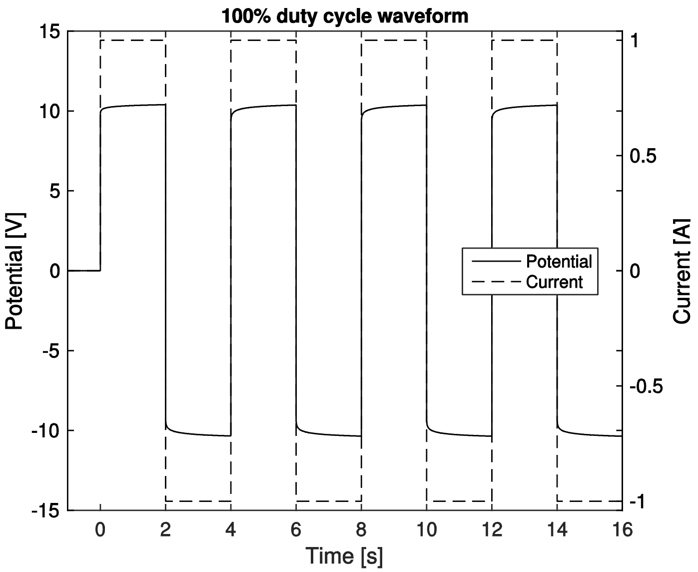

Figure 11. Showing injected current and modelled measured potential for the 100% duty-cycle waveform for time domain DCIP measurements.

The results show that on-time measurements of IP can reduce the acquisition time by up to 50% and increase the signal-to-noise ratio by up to 100% almost without information loss. The findings can contribute and have a large impact for DCIP surveys in general, and especially for surveys where time (and cost) efficiency and reliable data quality are important factors. Specifically, the findings are of value for DCIP surveys conducted in urban areas where anthropogenic noise is an issue and the heterogeneous subsurface demands time-consuming 3D acquisitions.

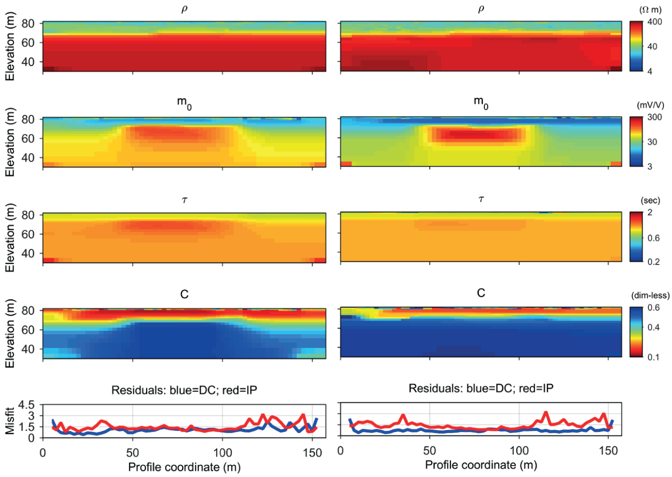

Figure 12. Inverted section and data misfit for field fata acquired with the 50% (left) and 100% (right) duty cycle current waveform.

4.2 Effect of current pulse on-time duration

These results concern the current injection duration and how this relates to resulting data, signal-to-noise ratio and inversion models.

The duration of time domain (TD) induced polarization (IP) current injections has significant impact on the acquired IP data as well as on the inversion models, if the standard evaluation procedure is followed. However, it is still possible to retrieve similar inversion models if the waveform of the injected current and the IP response waveform are included in the inversion. The on-time also generally affects the signal-to-noise ratio (SNR) where an increased on-time gives higher SNR for the IP data.

The commonly applied inversion of the induced polarization data only considers the integral chargeability, without taking the waveform of the injected current or the waveform of the IP response into account. The results show that, with these full waveform considerations included in the inversion, it is possible to retrieve similar inversion models for the induced polarization, independent of the on-time duration. Furthermore, the results show that the signal-to-noise ratio (SNR) for the IP information increases with increasing duration of the current injections.

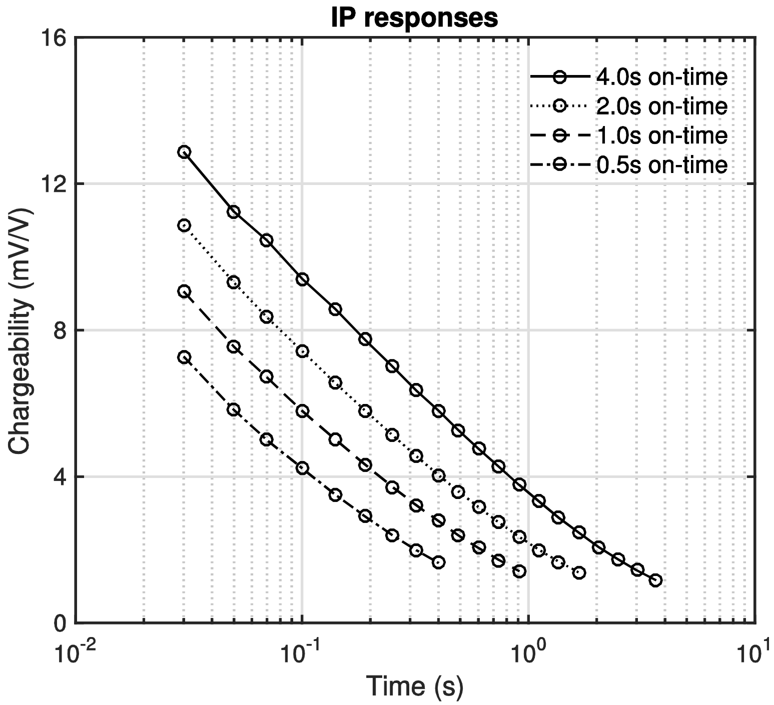

Figure 13. Acquired field IP decays corresponding to the same quadruple from each of the four data sets with different on- time. Note that the magnitude of the decays is increasing with longer on-time.

The results show that the on-time of the injected current has a substantial effect on retrieved induced polarization field data (Figure 13). It is clear from the results that this difference in data also affects the inverted subsurface IP models when using an inversion software that only considers integral chargeability Figure 14. However the results also show that it is in fact possible to retrieve similar inversion models given that the waveform of the injected current and the IP response waveform are included in the inversion (Figure 14) and that increasing on-time gives higher SNR for the IP data (Figure 13).

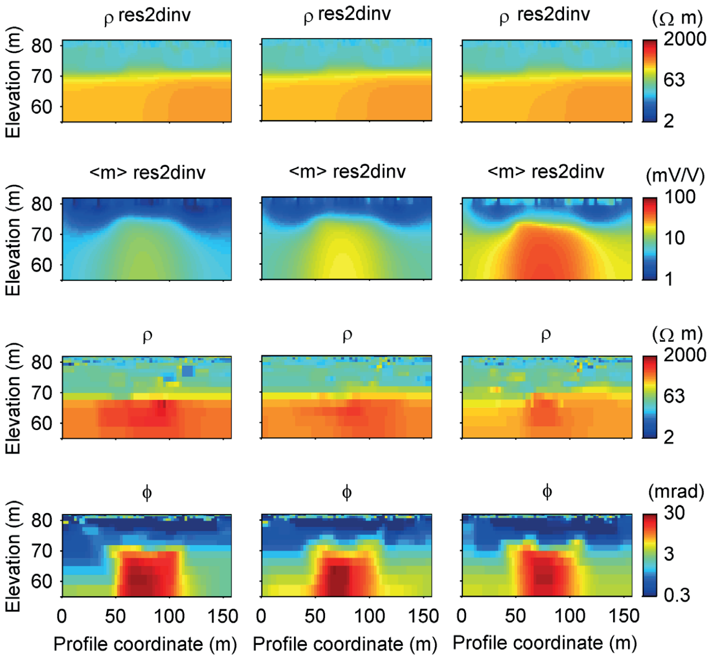

Figure 14. Inversion results from Res2dinv (two top rows) and Aarhusinv (two bottom rows) for different on-time (from left to right: 1, 2 and 4 seconds). The chargeability model from Res2dinv is clearly dependant on current on-time while the Aarhusinv (which include the current and potential waveforms in the inversion) models are more similar for the different on-times.

Only considering the integral chargeability can be misleading and likely makes it more ambiguous when trying to relate the IP models to processes and geology or preciously reported integral chargeability values. Furthermore, if not including the full waveform in the inversion, care needs to be taken that the same acquisition settings are used when making complimentary, verification or time-lapse measurements so that different data sets will be comparable in data and model space.

4.3 Signal processing of DCIP data

These results concern signal processing of full waveform DCIP data and handles measurement issues such as IP gate distribution, spikes, harmonic noise and background drift. The improved handling of these issues doubles the spectral information content of DCIP data by enabling shorter gates than the traditional method (multiple of the time period of the harmonic noise) and by accurately recovering the shape of the IP response at late times.

The normally used linear drift correction is for DC and integral chargeability measurements often good enough but when evaluating the spectral IP information a more accurate approximation is needed. This report here applies a Cole-Cole model based background drift estimate (Figure 15 and Figure 18, top) which substantially improves the handling of non-linear drift cases such as current induced electrode polarization and especially improves late times of the IP response with low signal-to-noise ratio.

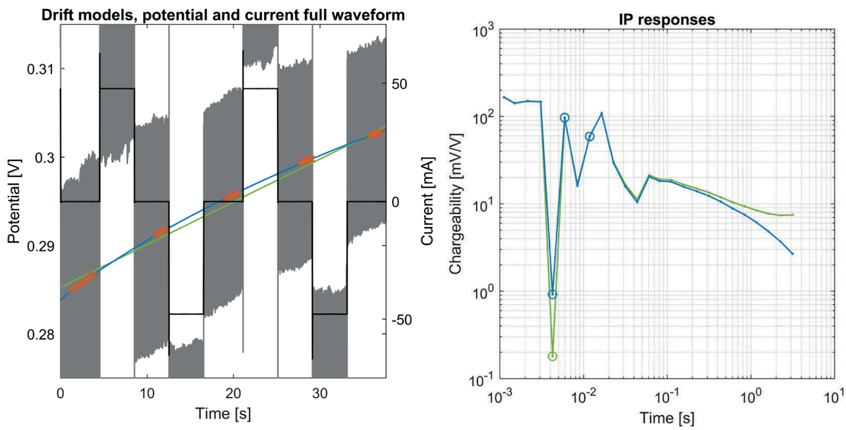

Figure 15. Showing 50% duty cycle raw full waveform potential (grey) and current (black), subset of the signal used for finding the drift model (red cross marker) and different types of background drift models (left). The resulting gated IP-response curves (green: linear model, blue: Cole-Cole model. Negative values are marked with circles) are shown in the top plot. Note that especially the end of the IP response is sensitive to the choice of drift model due to its low signal-to-noise ratio.

De-spiking is implemented by applying a series of filters on the full waveform potential for enhancing the spikes and generating a flexible and data-driven threshold value for spike rejection (Figure 16). The values of the identified spike samples are replaced based on the values of neighbouring non-spike samples.

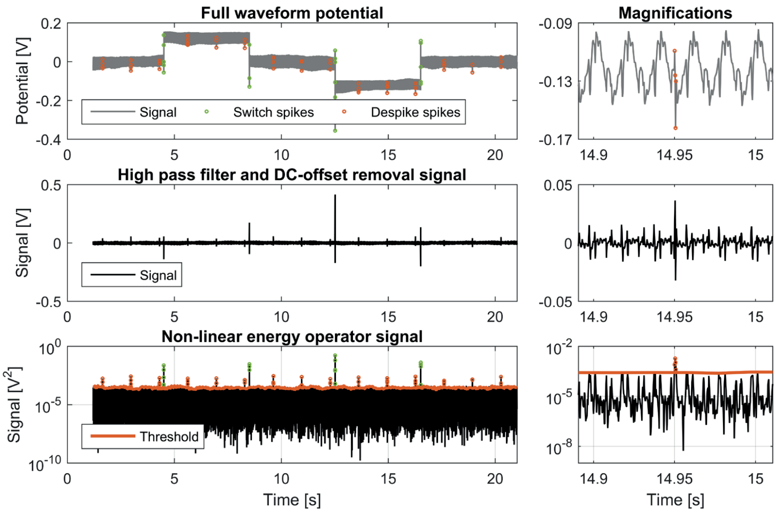

Figure 16. Showing identified spike samples of a full waveform potential signal (top), output from applied high pass and DC-offset removal filter (mid) and output from non-linear energy operator filter, spike samples and threshold value (bottom). Magnifications of the 7th identified despike spike (from 9.615 to 9.645 s) are shown on the right.

Cancelling of harmonic noise is implemented as a model based approach where the noise is described as a sum of harmonic signals. The different harmonic signals have frequencies given by a common fundamental frequency (f_0) multiplied with an integer (m) to describe the different harmonics but have independent amplitude (A_m) and phase (φ_m) for each harmonic m:

$$u_{harmonic\ noise}(n) = \sum_m A_m\, cos(2\pi m f_0 n + \varphi_m)$$

with sample number *n*.

Since the harmonic noise is not stationary for an entire data acquisition (varying in phase, amplitude and frequency), the raw full waveform potential is segmented. Noise model parameters are determined for each segment in an iterative approach by minimizing the residual energy after subtraction of a temporary harmonic noise model. After finding the best noise model, the raw full waveform potential is corrected accordingly, which substantially reduces the energy of the harmonic noise (Figure 17).

The model based cancelling of harmonic noise reduces the need for gating with multiples of 20 ms (for 50 Hz) to supress the harmonic noise. Hence an improved gate distribution design can be applied with arbitrary gate widths, both shorter than 20 ms and multiples of 20 ms when feasible. This design in turn gives access to spectral information of the IP response closer to time zero which were unavailable with the traditional gating (Figure 18). In total, the first useable gate is one decade in time closer to time zero with the improved gate distribution design and model based noise cancelling compared to when applying the traditional method for handling the harmonic noise.

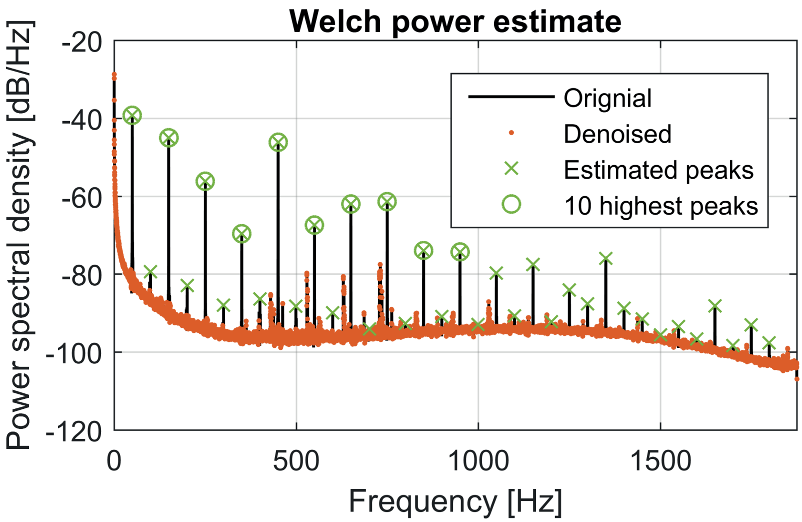

Figure 17. Welch power estimate of full waveform potential: original signal (black line), residual signal after noise cancellation (red dots). The green markers show identified energy peaks (cross) and harmonics used for finding the noise model (circle). The remaining energy peaks are not harmonics of the 50 Hz.

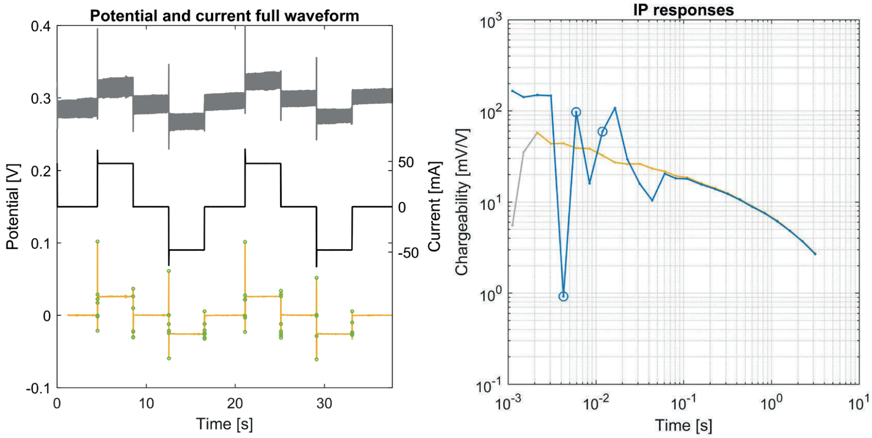

Figure 18. Showing full waveform current (black) and potential before (grey) and after (yellow) drift removal and cancelling of harmonic noise, switch spike samples are indicated by green o-marker (left). The resulting IP response with harmonic de-noising (right, yellow line. Gates associated with indicated switch spikes are shown in grey) shows clear improvement of the erratic behaviour of the IP response.

5 Conclusions

The work presented in this report demonstrates that the usefulness of the DCIP method can be improved. Field time and cost efficiency are increased by means of current pulse on-time and waveform optimization. Additionally, post processing efficiency increases as a result of improved data quality and reliability. Furthermore, the available spectral information from DCIP surveys is substantially increased by enabling extraction of the IP response closer to the pulse than was previously possible. In combination with more accurate removal of background drift potential that can handle non-linear drift cases, the data quality is improved at late times and the spectral information content is further increased.

This work has focused on time-domain resistivity and spectral IP measurements. However, it is still unclear if the time-domain measurements can resolve the spectral parameters equally well as the frequency domain counterpart. Furthermore, even if the work has substantially increased data quality for the spectral IP, it still demands extensive work of manual quality assurance and filtering of the IP response data to enable successful interpretations and inversions. Hence there is scope for further development related to data quality and data processing.

6 References

Argote-Espino, D., Tejero-Andrade, A., Cifuentes-Nava, G., Iriarte, L., Farías, S., Chávez, R.E., López, F., 2013. 3D electrical prospection in the archaeological site of El Pahñú, Hidalgo State, Central Mexico. Journal of Archaeological Science 40, 1213–1223. doi:10.1016/j.jas.2012.08.034

Auken, E., Doetsch, J., Fiandaca, G., Christiansen, A.V., Gazoty, A., Cahill, A.G., Jakobsen, R., 2014. Imaging subsurface migration of dissolved CO2 in a shallow aquifer using 3-D time-lapse electrical resistivity tomography. Journal of Applied Geophysics 101, 31–41. doi:10.1016/j.jappgeo.2013.11.011

Auken, E., Pellerin, L., Christensen, N.B., Sørensen, K., 2006. A survey of current trends in near-surface electrical and electromagnetic methods. Geophysics 71, 249–260. doi:10.1190/1.2335575

Binley, A., 2015. Tools and Techniques: Electrical Methods, in: Treatise on Geophysics. Elsevier, pp. 233–259. doi:10.1016/B978-0-444-53802-4.00192-5

Butler, D.K., 2005. Near-surface geophysics. Society of Exploration Geophysicists Tulsa.

Dahlin, T., 2001. The development of DC resistivity imaging techniques. Computers & Geosciences 27, 1019–1029.

Dahlin, T., Bjelm, L., Svensson, C., 1999. Use of electrical imaging in site investigations for a railway tunnel through the Hallandsås Horst, Sweden. Quarterly Journal of Engineering Geology & Hydrogeology 32, 163–173.

Dahlin, T., Leroux, V., 2012. Improvement in time-domain induced polarization data quality with multi-electrode systems by separating current and potential cables. Near Surface Geophysics 10, 545–656. doi:10.3997/1873-0604.2012028

Dahlin, T., Leroux, V., Nissen, J., 2002. Measuring techniques in induced polarisation imaging. Journal of Applied Geophysics 50, 279–298. doi:10.1016/S0926-9851(02)00148-9

Dahlin, T., Rosqvist, H., Leroux, V., 2010. Resistivity-IP mapping for landfill applications. First Break 28.

Doetsch, J., Fiandaca, G., Auken, E., Christiansen, A.V., Cahill, A.G., 2015a. Field-scale time-domain spectral induced polarization monitoring of geochemical changes induced by injected CO2 in a shallow aquifer. Geophysics 16, 10294. doi:10.1190/geo2014-0315.1

Doetsch, J., Ingeman-Nielsen, T., Christiansen, A. V., Fiandaca, G., Auken, E., Elberling, B., 2015b. Direct current (DC) resistivity and induced polarization

(IP) monitoring of active layer dynamics at high temporal resolution. Cold Regions Science and Technology 119, 16–28. doi:10.1016/j.coldregions.2015.07.002

Fetter, C.W., 2001. Applied hydrogeology. Prentice Hall, Upper Saddle River N.J.

Fiandaca, G., Auken, E., Christiansen, A.V., Gazoty, A., 2012. Time-domain-induced polarization: Full-decay forward modeling and 1D laterally constrained inversion of Cole-Cole parameters. Geophysics 77, E213–E225. doi:10.1190/geo2011-0217.1

Fiandaca, G., Ramm, J., Binley, A., Gazoty, A., Christiansen, A.V., Auken, E., 2013. Resolving spectral information from time domain induced polarization data through 2-D inversion. Geophysical Journal International 192, 631–646. doi:10.1093/gji/ggs060

Fink, J.B., 1990. Induced polarization: applications and case histories. Soc of Exploration Geophysicists.

Florsch, N., Llubes, M., Téreygeol, F., Ghorbani, A., Roblet, P., 2011. Quantification of slag heap volumes and masses through the use of induced polarization: application to the Castel-Minier site. Journal of Archaeological Science 38, 438–451. doi:10.1016/j.jas.2010.09.027

Gazoty, A., Fiandaca, G., Pedersen, J., Auken, E., Christiansen, A. V., Pedersen, J.K., 2012a. Application of time domain induced polarization to the mapping of lithotypes in a landfill site. Hydrology and Earth System Sciences 16, 1793–1804. doi:10.5194/hess-16-1793-2012

Gazoty, A., Fiandaca, G., Pedersen, J., Auken, E., Christiansen, A. V, 2012b. Mapping of landfills using time-domain spectral induced polarization data: The Eskelund case study. Near Surface Geophysics 10, 575–586. doi:10.3997/1873-0604.2012046

Gazoty, A., Fiandaca, G., Pedersen, J., Auken, E., Christiansen, A. V, 2013. Data repeatability and acquisition techniques for time-domain spectral induced polarization. Near Surface Geophysics 391–406. doi:10.3997/1873-0604.2013013

Glover, P.W.J., 2015. Geophysical Properties of the Near Surface Earth: Electrical Properties, Treatise on Geophysics. Elsevier B.V. doi:10.1016/B978-0-444-53802-4.00189-5

Günther, T., Rücker, C., Spitzer, K., 2006. Three-dimensional modelling and inversion of dc resistivity data incorporating topography - II. Inversion. Geophysical Journal International 166, 506–517. doi:10.1111/j.1365-246X.2006.03011.x

Hönig, M., Tezkan, B., 2007. 1D and 2D Cole-Cole-inversion of time-domain induced-polarization data. Geophysical Prospecting 55, 117–133.

doi:10.1111/j.1365-2478.2006.00570.x

Ingeman-Nielsen, T., Baumgartner, F., 2006. Numerical modelling of complex resistivity effects on a homogenous half-space at low frequencies. Geophysical Prospecting 54, 261–271. doi:10.1111/j.1365-2478.2006.00532.x

Johnson, I.M., 1984. Spectral induced polarization parameters as determined through time-domain measurements. Geophysics 49, 1993–2003. doi:10.1190/1.1441610

Kemna, A., Binley, A., Slater, L., 2004. Crosshole IP imaging for engineering and environmental applications. Geophysics 69, 97–107. doi:10.1190/1.1649379

Leroux, V., Dahlin, T., 2005. Time-lapse resistivity investigations for imaging saltwater transport in glaciofluvial deposits. Environmental Geology 49, 347–358. doi:10.1007/s00254-005-0070-7

Leroux, V., Dahlin, T., Svensson, M., 2007. Dense resistivity and induced polarization profiling for a landfill restoration project at Harlov, Southern Sweden. Waste Management & Research 25, 49–60. doi:10.1177/0734242X07073668

Loke, M.H., Barker, R.D., 1996. Practical techniques for 3D resistivity surveys and data inversion1. Geophysical Prospecting 44, 499–523. doi:10.1111/j.1365-2478.1996.tb00162.x

Loke, M.H., Chambers, J.E., Rucker, D.F., Kuras, O., Wilkinson, P.B., 2013. Recent developments in the direct-current geoelectrical imaging method. Journal of Applied Geophysics 95, 135–156. doi:10.1016/j.jappgeo.2013.02.017

Nijland, W., van der Meijde, M., Addink, E.A., de Jong, S.M., 2010. Detection of soil moisture and vegetation water abstraction in a Mediterranean natural area using electrical resistivity tomography. CATENA 81, 209–216. doi:10.1016/j.catena.2010.03.005

Pelton, W.H., Ward, S.H., Hallof, P.G., Sill, W.R., Nelson, P.H., 1978. Mineral discrimination and removal of inductive coupling with multifrequency IP. Geophysics 43, 588–609. doi:10.1190/1.1440839

Peter-Borie, M., Sirieix, C., Naudet, V., Riss, J., 2011. Electrical resistivity monitoring with buried electrodes and cables: noise estimation with repeatability tests. Near Surface Geophysics 9, 369–380. doi:10.3997/1873-0604.2011013

Radic, T., 2004. Elimination of Cable Effects while Multi-Channel SIP Measurements, in: Near Surface 2004 - 10th EAGE European Meeting of Environmental and Engineering Geophysics.

Revil, A., Binley, A., Mejus, L., Kessouri, P., 2015. Predicting permeability from the characteristic relaxation time and intrinsic formation factor of complex conductivity spectra. Water Resources Research 51, 6672–6700.

doi:10.1002/2015WR017074

Rücker, C., Günther, T., Spitzer, K., 2006. Three-dimensional modelling and inversion of dc resistivity data incorporating topography - I. Modelling. Geophysical Journal International 166, 495–505. doi:10.1111/j.1365-246X.2006.03010.x

Seigel, H.O., 1959. Mathematical formulation and type curves for induced polarization. Geophysics 24, 547–565. doi:10.1190/1.1438625

Slater, L., Ntarlagiannis, D., Yee, N., O'Brien, M., Zhang, C., Williams, K.H., 2008. Electrodic voltages in the presence of dissolved sulfide: Implications for monitoring natural microbial activity. Geophysics. doi:10.1190/1.2828977

Slater, L.D., Glaser, D.R., 2003. Controls on induced polarization in sandy unconsolidated sediments and application to aquifer characterization. Geophysics. doi:10.1190/1.1620628

Slater, L.D., Lesmes, D., 2002. IP interpretation in environmental investigations. Geophysics 67, 77. doi:10.1190/1.1451353

Sumner, J.S., 2012. Principles of induced polarization for geophysical exploration. Elsevier.

Tombs, J.M.., 1981. The feasibility of making spectral IP measurements in the time domain. Geoexploration 19, 91–102. doi:10.1016/0016-7142(81)90022-3

Zonge, K.L., Wynn, J., Urquhart, S., 2005. 9. Resistivity, Induced Polarization, and Complex Resistivity, in: Near-Surface Geophysics. pp. 265–300. doi:10.1190/1.9781560801719.ch9

Box 5501
SE-114 85 Stockholm

info@befoonline.org • www.befoonline.org
Visiting address: Storgatan 19, Stockholm

ISSN 1104-1773